ISIJ International, Vol. 33 (1993), No. 5, pp. 567–576

Fe–Cr Melt Nitrogenation When Exposed to Nitrogen Plasma

O. P. SINHA and R. C. GUPTA

Department of Metallurgical Engineering, Institute of Technology, Banaras Hindu University, Varanasi-221 005, India.

(Received on November 9, 1992; accepted in final form on February 25, 1993)

The nitrogen absorption/desorption for pure iron and Fe–C alloys have been investigated in detail in levitated melts. However, limited study seems to be made while molten Fe–Cr alloy is exposed to nitrogen plasma. Nitrogen plasma offers an attractive means to nitrogenise Fe–Cr alloys in view of rapid absorption to higher nitrogen content. Several workers have reported that sulphur in the melt renders higher nitrogen. Industrially melt with higher nitrogen with sulphur may not be attractive. The experimental condition of present study solves this problem. Melts were made to observe the effect of arc current, plasma gas composition, surface active elements (SAE) in melt on melt nitrogen content. It was noted that the nitrogen was first absorbed upto certain maximum limit [N_{max}] followed by its desorption on continued plasma exposure may be due to nitrogen bubble formation. The maximum nitrogen level in melts could be enhanced when rate of absorption in plasma arc zone was much higher with low desorption occurring in non-plasma arc zone of the melt. The use of higher melt temperature and low SAE in melt rendered higher absorption rate. The slower desorption rate could be obtained by maintaining lower SAE and temperature in melts. The nitrogen absorption in plasma arc zone followed first order reaction rate, however, desorption was probably depended on bubble formation frequency.

KEY WORDS: nitrogenation; nitrogen plasma; Fe–Cr melt; stainless steel; temperature; ac plasma; SAE; absorption; desorption.

1. Introduction

Nitrogen absorption and desorption has been a subject of great interest for quite some time due to various harmful/beneficial effects[1] caused by it in different melt systems. Battle and Pehlke[2] reviewed the work done in the past quarter of a century and concluded that absorption into high purity iron is of first order and limited by liquid phase mass transfer. As the surface active elements such as oxygen and sulphur are added to the liquid iron, the reaction rates decrease and eventually become second order. This second order effect is due to the increasing significance of interfacial chemical reaction control. Recently Cho and Rao[3] studied the rate of absorption for iron–chromium alloys in levitated condition. Literature survey reveals that many studies have been carried out using pure iron or iron–carbon alloys whereas only a few studies have been reported on iron–chromium system. Further, such studies were conducted using various melt techniques, *e.g.*, resistance heating,[4–7] induction heating,[8–16] levitation melting[3,8,9,17–22] and plasma arc melting.[19,23–26] Amongst these melting techniques, studies reported for nitrogenation of Fe–Cr alloy using plasma arc are very limited. In view of various advantages[27–32] of plasma arc system, its application for preparing nitrogen bearing iron–chromium alloys is expected to increase. The beneficial properties of nitrogen in stainless steel is well established.[32–36]

Plasma arc is electrically conductive while being electrically neutral since plasma is a highly ionized gas containing positive ions and electrons in equal number. When molten metal is exposed to plasma arc, nitrogen absorption is believed to take place only in arc zone,[26] where ionized nitrogen is rapidly absorbed by the metal, whereas, outside this zone all nitrogen occurs in molecular form. In contrast to this, desorption seems to take place in non-plasma area. The bulk metal will contain retained nitrogen after desorption. In plasma arc zone, melt nitrogen content is higher[23] than the bulk metal equilibrium nitrogen content due to ionic nature of nitrogen. The nitrogen solubility limit in Fe–Cr melts would depend on its alloy composition, nitrogen partial pressure and temperature, whereas the rate of absorption/desorption depends on the presence of surface active elements (S, O and Se), nitrogen partial pressure, melt temperature, melt movement, crucible material *etc.* Kemeny *et al.*[19] observed higher nitrogen in carbon saturated iron melt, exposed to nitrogen plasma when the sulphur content in the melt was increased. Takeda *et al.*[23] also found higher nitrogen in melt with increasing sulphur content while studying nitrogen behaviour of pure iron under nitrogen plasma arc. Katz and King[26] have reported that the rate of nitrogen desorption is low at higher sulphur level of pure iron melt resulting into higher melt nitrogen content. These observations though logical would appear discouraging for achieving higher nitrogen in stainless steel melt with low sulphur content

which would be needed industrially.

The present study aimed to produce high nitrogen Fe–Cr alloys with low sulphur content using nitrogen plasma. The experiments were designed to study nitrogen absorption by commercial purity Fe–Cr melt exposed to nitrogen plasma arc (ac) as affected by exposure time, melt temperature, quantity of Cr, Mn, Ni, SAE and arc gas composition [N_2–Ar].

2. Experimental

2.1. Material

Commercial purity iron (98.5% Fe, 0.9% Mn, 0.29% Si, 0.2% C, 0.008% Al, 0.02% S, 0.104% O, 0.0044% N), armco iron, ferro-chrome (31.68% Fe, 68.0% Cr, 0.083% C, 0.0527% N, 0.185% O), nickel (99.03% Ni), manganese (99.7% Mn, 0.010% C, 0.265% O, 0.0056% N) and commercial purity gases (Nitrogen and Argon) were used for the experiments.

2.2. Equipment

A 30 kVA ac-plasma arc furnace (**Fig. 1**) was used in this work. This unit was indigeneously designed and fabricated.[37] The burnt magnesite granules and powder mix was used as refractory lining for crucible and roof. The drilled graphite rod (0.016 mϕ) served as electrode. The furnace had common port for charging, viewing and sampling. The temperature was monitored continuously by radiation pyrometer and checked periodically by immersion (Pt–Pt/13%Rh) pyrometer. It rested on trunions for easy pouring and had lift-swing type roof cover. The equipment had no automation and every operation was manually controlled.

2.3. Melting Condition

The melt area to volume was 0.20 cm^{-1} for 2 kg melt with presently used crucible geometry and no induction coil was provided around crucible for melt stirring or heating.

2.4. Melting Procedure

The 2 kg charge (iron, ferro-chrome and nickel) was weighed in desired proportion to get alloys of desired composition (*e.g.*, 75%Fe–20%Cr–5%Ni). The iron was charged in the furnace, melted under normal arc, alloying additions were made and melt homogenized. The melt was then deoxidised by adding ferrosilicon followed by alloying additions. The bulk melt temperature was checked with Pt–Pt/13Rh dip type thermocouple and a pin sample was sucked out with the help of especially designed silica pipette to know its initial composition. Subsequently the melt was exposed to nitrogen plasma and samples taken out at every 30 s interval upto 300 s. During this period, the melt temperature was continuously recorded through radiation pyrometer. After 300 s plasma exposure, the melt was poured into a metallic mould to obtain a cast ingot having 125 mm × 75 mm × 25 mm size.

2.5 Analysis

The samples taken out at various stages were analysed for nitrogen and oxygen contents using Leco model TC-236 whereas for carbon and sulphur contents Leco model CS-244 was used. The final melt was analysed for all the constituents using X-ray Fluorescence Spectrometer analyser (XRF model MRS 400).

3. Results

3.1. Effect of Plasma Exposure Time

Figure 2 shows the nitrogen content of a typical melt (15.6% Cr and 4.65% Ni) with increasing plasma exposure time. In this experiment 247 A current and 100% nitrogen gas (8.33×10^{-6} m^3/s) for plasma arc were used. The initial nitrogen content of the melt was determined to be 0.1358%. This nitrogen was picked up by the melt from the atmosphere because the melt had to be heated after alloying using normal arc. This was unavoidable as total weight of the charge was 2 kg and some heating period was found to be essential after alloying. Such temperature adjustments may not be needed while practising on tonnage scale or when an auxiliary induction coil is provided for stirring and heating.

On exposure to nitrogen plasma, the nitrogen content in the melt was found increased to 0.1984% with time (120 s) but with continued exposure, it decreases to 0.1444% (at 300 s) (Fig. 2). During this period (300 s),

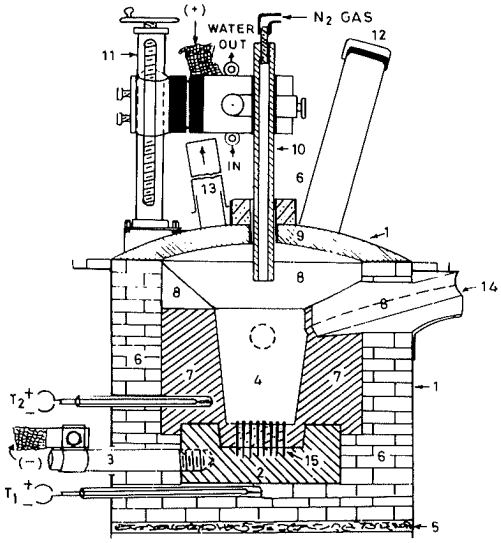

Fig. 1.
Laboratory plasma arc furnace (3 kg capacity).

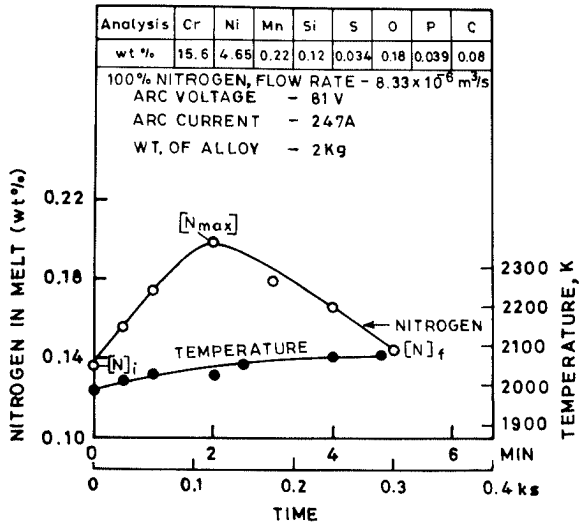

Fig. 2. Effect of nitrogen plasma arc exposure time on melt nitrogen content and temperature.

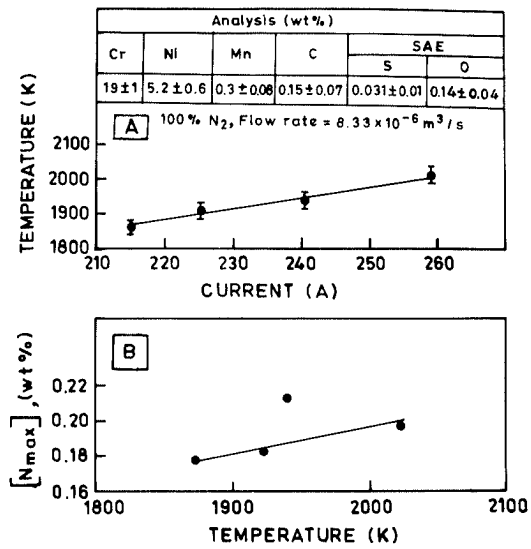

Fig. 3. (A) Effect of plasma arc current on melt temperature.
(B) Effect of melt temperature on melt nitrogen conent $[N_{max}]$.

the melt temperature was also noticed to increase from 1 973 to 2 073 K. Further, it was also observed that the melt started bubbling after about 120–150 s time.

As reported by others[26] it appears that the nitrogen is absorbed in the arc zone by the melt and it gets desorbed simultaneously from the remaining melt area. Thus, at any given moment, melt nitrogen is the balance of nitrogen absorbed in arc zone and nitrogen desorbed in non arc zone. It seems that during the initial period, the rate of absorption outweighs the desorption rate resulting in increasing nitrogen content. It ceases to increase when absorption equalies desorption and the melt attains a steady state after certain period as experienced by Kemeny *et al.*[19] However, the present observations show no such steady state. The decreasing nitrogen content after certain time indicates that desorption rate is perhaps faster than absorption after a certain period.

Similar behaviour was also noticed in other melts of this investigation. Thus, for introducing a specific nitrogen content, it is essential to know the parameters, which control the rate of absorption and desorption such that appropriate exposure time could be estimated and hence fixed for obtaining a desired nitrogen level in the melt. Before analysing the parameters controlling the rate of absorption or desorption, the effects of other parameters on maximum nitrogen content $[N_{max}]$ attained by the melt are described in the following sections.

3.2. Effect of Arc-current Intensity and Type

A few melts were made with increasing arc current from 215 to 260 A. The melts had nearly the same amounts of alloying elements (19±1% Cr, 5.2±0.6% Ni) and impurities (0.17±0.05% SAE). The plasma gas contained 100% nitrogen (8.33×10^{-6} m^3/s). The nitrogen content in the melt and melt temperature profile in all such melts were similar to that shown in Fig. 2. However, it was observed that $[N_{max}]$ and corresponding melt temperature were different in such cases. **Figure 3(A)** shows increase in melt temperature with arc current, which results in increased $[N_{max}]$ (**Fig. 3(B)**). It is inter-

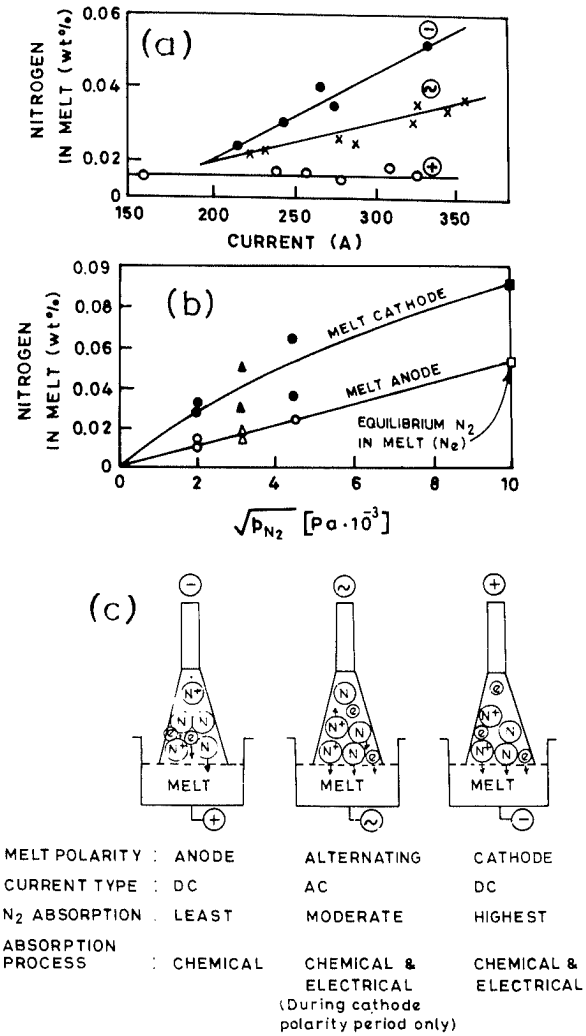

Fig. 4. (a) Final nitrogen content of melt as affected by current type, polarity and intensity (after V. Dembovsky).[38]
(b) Dependences of the nitrogen content on the partial pressure of nitrogen while melt being cathode and anode in dc-plasma (after V. Dembovsky).[38]
(c) Effect of melt polarity on nitrogen absorption–Schematic view.

esting to note that a similar result has been reported by Podgayetski *et al.* (**Fig. 4(a)**, cited from Dembovsky).[38]

Dembovsky[38] has tried to differentiate chemical absorption (dissolution) with and without applied electrical field when the melt is made cathode and anode, respectively, using dc current. In such studies, when the melt is made anode, the chance of positively charged ions N^+ being adsorbed will be low and may be confined to chemical dissolution of neutral ions N only resulting in maximum nitrogen equal to equilibrium value (**Fig. 4(b)**). On the other hand when the melt acts as cathode, the total nitrogen in melt can exceed equilibrium value due to the absorption of positively charged ions N^+, N^{++} by melt cathode (electrical absorption) in addition to chemical dissolution of neutral ions N. In ac plasma, the $[N_{max}]$ lies in between the two values (Fig. 4(a)) obtained in dc plasma on account of polarity reversal. The present case belongs to ac plasma and hence the absorption (dissolution) is considered to be due both chemical and electrical absorption. Such a concept is shown schematically in **Fig. 4(c)**. Thus the $[N_{max}]$ observed in these experiments was marginal (1.1 times) in excess of equilibrium nitrogen compared to that reported in studies[19,23,26] using dc plasma (6 to 100 times excess nitrogen). It may be pointed out that the lower pick up of excess nitrogen may also be due to the fact that a good proportion of the excess nitrogen bubbles out as confirmed by heavy boiling observed during melting period. Such was not the case in the experiments conducted by Kemeny *et al.*,[19] Takeda and Nakamura,[23] and Katz and King.[26]

3.3. Effect of Nitrogen Content in Plasma Gas

Two melts were prepared using 20 and 80% nitrogen mixed with argon for plasma gas. The melts contained 21.8 ± 0.4% Cr and 5.4 ± 0.4% Ni with total SAE amounting to about 0.10 ± 0.008%. The melt temperature was $1\,900\pm20$ K. From **Fig. 5**, it is evident that $[N_{max}]$ values are practically unaffected by nitrogen partial pressure.

Blake and Jordan[39] found that the increasing percentage of nitrogen (0–1%) in arc atmosphere resulted in increased nitrogen absorption rate in weld melts following Sievert's law, however, Death and Haid[40] reported that higher nitrogen partial pressure beyond 0.27 atm did not yield increased nitrogen in molten iron alloys.

Kemeny *et al.*[19] also observed that an increase in nitrogen partial pressure upto 0.2 atm causes a proportional rise in number of activated, ionised and atomic nitrogen species. They stated that at higher nitrogen partial pressures, the gas boundary layer seems to be saturated at the interface and hence a further increase of nitrogen in plasma has no effect. At higher partial pressures of nitrogen (>0.2 atm), mass transport in the bulk liquid may be rate controlling. Similar observations have also been reported by Gallardo *et al.*[7] and Bhat.[41]

3.4. Effect of Melt Alloying Elements

In order to study the effect of alloying elements (Cr, Mn and Ni), several melts were made using 100% N_2 gas for plasma. The melt temperatures in such cases were around $1\,920\pm20$ K and the SAEs were restricted to 0.14 ± 0.08 wt%. The $[N_{max}]$ values of the melts are shown in **Fig. 6** against the addition in the Fe–Cr or Fe–Ni alloys.

It was observed that Cr and Mn addition increased the $[N_{max}]$ values whereas it decreased with Ni. These observations are in agreement with the literature.[42–44]

3.5. Effect of Surface Active Elements

In order to observe the effect of surface active elements, such as sulphur and oxygen, in the melt on the melt $[N_{max}]$ value, a few melts were prepared. The melt oxygen content could be decreased by increasing the quantity of deoxidiser (ferrosilicon) whereas oxygen was used to increase its value in some cases. The melt sulphur content could be controlled by adding armco iron or iron sulphide as required. In such melts, 19 ± 1 wt% Cr and 5.2 ± 0.6 wt% Ni were added. The melt temperature was maintained around $1\,900\pm20$ K. The $[N_{max}]$ value of the

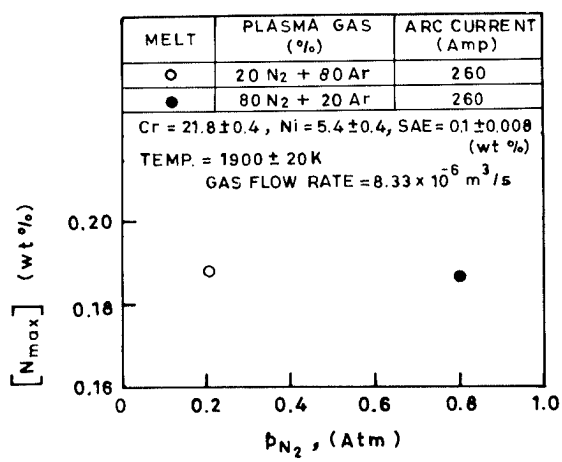

Fig. 5. Effect of partial pressure of nitrogen in plasma gas on melt nitrogen content $[N_{max}]$.

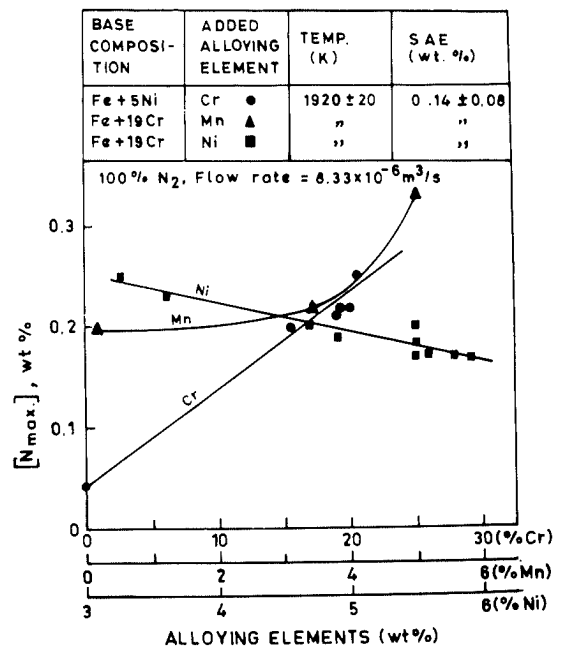

Fig. 6. Effect of chromium, manganese and nickel on $[N_{max}]$ content in melt during plasma arc exposure.

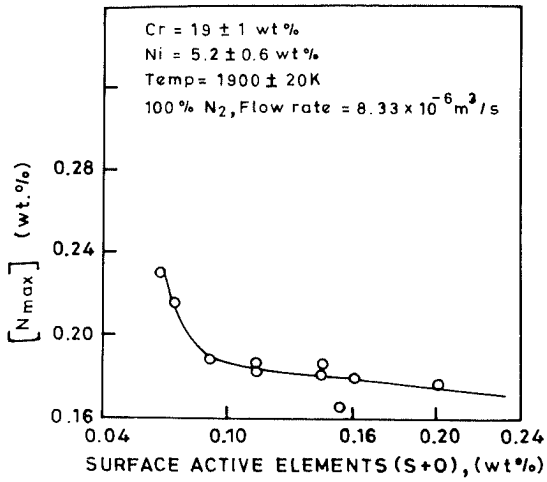

Fig. 7. Effect of SAE on maximum nitrogen content [N_{max}] in melt.

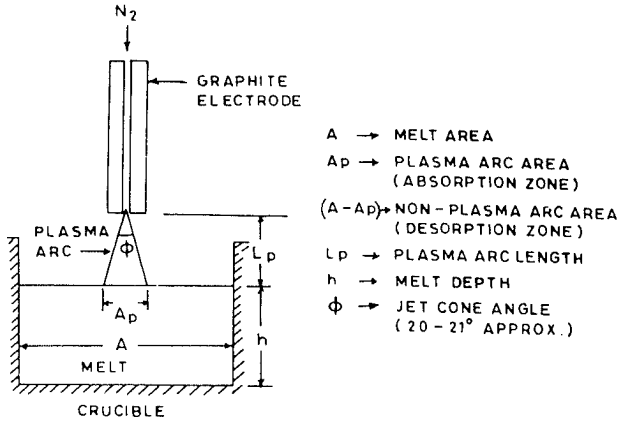

Fig. 8. Schematic diagram showing plasma arc zone for absorption and remaining non-arc zone for desorption of nitrogen.

melts observed during 300 s of plasma exposure time is plotted against total SAE in the melt (**Fig. 7**). It is obvious that the [N_{max}] decreased with increase in SAE. This is in contrast to that reported by Kemeny *et al.*[19] (Takeda and Nakamura[23] and also Katz and King[26]) and is attributed to the difference in experimental conditions. Free nitrogen bubble formation and evolution were possible in these studies whereas it was not reported in the earlier investigations using high pressure[23] or melt stirring.[19] The effect of formation of bubble will be explained in a subsequent section. It may be pointed out here that sulphur is known to be an undesirable element because it impairs the mechanical properties of the alloy.[45] The experimental conditions employed here favour higher nitrogen content with reduced sulphur and oxygen content, which is a desirable condition for plant practice.

4. Discussion

4.1. Melt Nitrogen Content

The foregoing observations indicated that high values of [N_{max}] can be promoted by having conditions conducive to high nitrogen solubility. The said objective can be attained by optimising alloying element additions (*e.g.*, high Cr, Mn and low Ni), low SAEs (O+S), adequate temperature, proper p_{N_2} in the plasma and appropriate time of exposure.

In gas/metal reactions, generally, gas absorption and desorption proceed simultaneously. Unlike other gas/metal exposure techniques where absorption (or adsorption)/desorption occur over the entire melt area, in plasma arc nitrogenation method there seem to be two distinct area zones as illustrated in **Fig. 8**. It is generally believed[26] that absorption (or adsorption) takes place in plasma arc zone (A_p) whereas desorption occurs through remaining (non-plasma) zone ($A-A_P$). The A_P zone will depend mainly on arc length (L_P), electrode bore diameter and gas flow rate, which can be calculated by taking air jet cone angle (ϕ)[46-48] and has been reported to vary from 20 to 21°. It may be noted even here that the thermal status [*i.e.*, *in situ* temperatures of those two zones] can be substantially different resulting respectively in relatively a stirred zone (A_P) and a quiscent zone ($A-A_P$). Hence, the rate of absorption (or adsorption) is likely to be rapid in the zone A_P and slower desorption over the wider non-plasma area ($A-A_P$) of the melt. The net nitrogen dissolved in melt will therefore be a balance of total nitrogen adsorbed in arc zone and desorbed from the non-arc zone.

4.2. Nitrogen Absorption Rate

The process of nitrogen absorption can be broken down into following steps:

(1) Rate of supply of nitrogen to gas boundary layer which is dependent on the p_{N_2} of the plasma.

(2) Mass transport of the nitrogen species through gas boundary layer

(3) Chemical reaction at gas melt interface inclusive of adsorption

(4) Mass transport of N through the melt boundary layer.

Of these four steps, the first two steps can be ignored because excess supply of nitrogen is found to be noneffective in influencing the nitrogen content of the melt (Fig. 5).

It is mostly[3,4,9-12,14,19] agreed that nitrogen dissolution follows first order kinetics which may be represented as:

$$-\frac{dN}{dt}=K_a\frac{A_P}{V}(N_e-N) \quad \text{.....(1)}$$

where, K_a = Apparent rate constant for absorption (or adsorption) (m/s)
A_P = Absorption surface area (Arc zone) (m^2)
V = Volume of the melt (m^3)
N_e = Equilibrium nitrogen concentration for the specified nitrogen pressure (wt%)
N = Nitrogen concentration at any time (wt%)

Integrating Eq. (1), we get,

$$-\ln\left[\frac{N_e-N_i}{N_e-N_t}\right]=K_a\frac{A_P}{V}t \quad \text{.....(2)}$$

where, N_i = Initial nitrogen concentration (wt%)
N_t = Final nitrogen concentration at time t s (wt%)

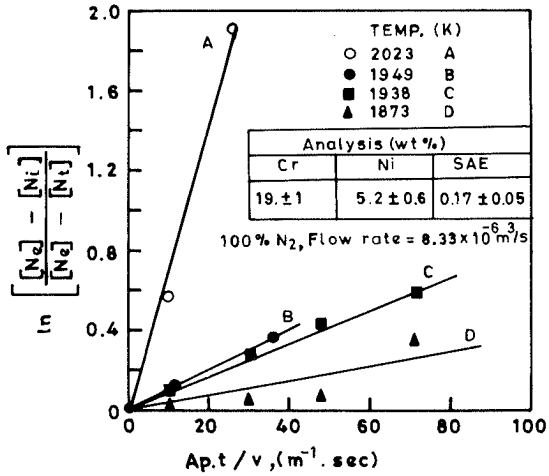

Fig. 9. Absorption by melt in plasma arc zone according to 1st order reaction control.

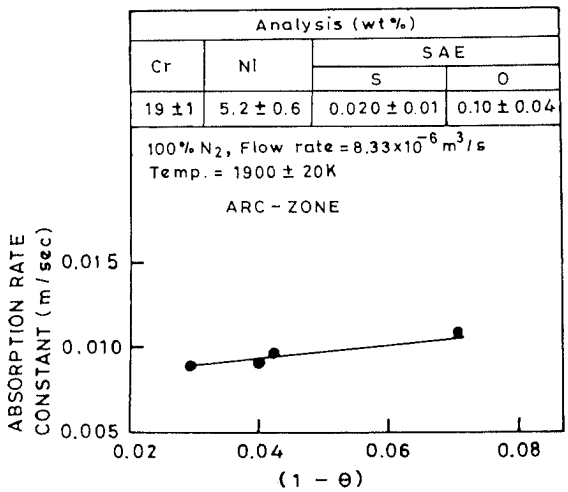

Fig. 10. Effect of free active sites on nitrogen absorption rate by melt.

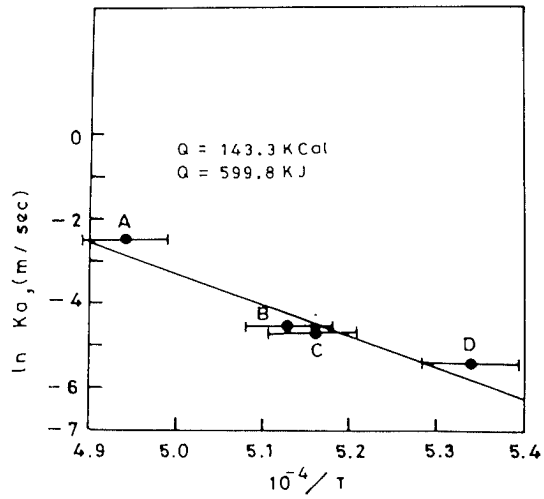

Fig. 11. Arrhenius plot indicating temperature dependence of absorption rate constant.

Table 1. Activation energy for nitrogen absorption in molten iron and iron-alloys.

Ref.	Investigators	System	SAE* (wt%) S	SAE* (wt%) O	Activation energy (kcal)
11)	Inouye and Choh	Pure Iron	—	—	10–12 (k_1)
10)	Pehlke and Elliotte	Iron	—	0.05	45.0 (k_1)
9)	Rao and Lee	Iron	0.0012	—	24.5 (k_1)
		Iron	0.27	—	108.6 (k_2)
49)	Byrne and Belton	Pure iron	—	—	34.7 (k_1)
3)	Cho and Rao	Fe–10Cr	0.002	—	19.4 (k_1)
		—do—	0.25	—	56.0 (k_2)
	Present work	Fe–20Cr–5Ni	(0.04 ±0.02)	(0.13 ±0.03)	~143.0 (k_1)

* SAE: Surface Active Elements.
k_1 = 1st order rate constant (m/s), k_2 = 2nd order rate constant (m/%-s)

A linearity of the $\ln[(N_e-N_i)/(N_e-N_t)]$ against $(A_p t/V)$ plot (**Fig. 9**) confirms that results of the present work fit into a first order reaction rate expression.

These rate constant (K_a) values are seen to be strongly influenced by the presence of surface active elements (SAE), *e.g.*, sulphur, oxygen and selenium. The SAEs presumably occupy some of the reaction sites and retard the adsorption rate. From the concept of Langmuir adsorption kinetics applicable to such surface reactions (gas/liquid), an expression for free sites $(1-\theta)$ can be derived as was done by Hua and Parlee[16] giving satisfactory results even for alloyed melts:

$$(1-\theta)=\frac{1}{1+K_o a_o+K_s a_s} \quad \text{.....(3)}$$

where, K_o and K_s: adsorption rate constants for oxygen (160) and sulphur (140) respectively at 1 873 K,

a_o and a_s: activity of oxygen and sulphur in melt respectively. At low concentrations, one can take wt% concentration equal to its activity.[16]

Using Eq. (3), the free surface fraction $(1-\theta)$ was calculated since S% and O% for all the samples were known. The apparent adsorption rate (K_a) constant values for a few melts were plotted against $(1-\theta)$. **Figure 10** indicates increasing rate of nitrogen adsorption with higher $(1-\theta)$ values. Thus, nitrogen absorption appears to be controlled by chemical reaction. The increased absorption with low SAE in melt observed in this study is in agreement with that reported by some researchers.[2,3,9–12,16,17]

The higher values of rate constant observed in the present studies reflect the rapid absorption under ac plasma arc where chemical reaction is aided by electrical absorption.

The temperature of the melt will undoubtedly influence the rate of nitrogen pick-up.

It was difficult to regulate the melt temperature in the manually controlled plasma arc system, but the melt temperature is considered reliable within ±20 K. The $\ln K_a$ values plotted against $[1/T\,(\mathrm{K})]$ and shown in **Fig. 11** (using Fig. 9 data), indicate the observance of an Arrhenius relationship. From the slope of the said straight line relationship, the approximate value (due to wide range of SAE 0.12–0.22 wt% and temprature

± 20 K) of activation energy has been calculated to be 600 kJ (143 kcal). It is compared with the results of earlier investigations on other alloys in **Table 1**. In the absence of any reported activation energy value for the alloys under study in plasma arc system, it is difficult to comment on this aspect.

4.3. Nitrogen Desorption Rate

The gas desorption from melt may be represented by:

$$2[N] = N_2(g) \quad \text{.....(4)}$$

The above is a second order equation whose rate expression is:

$$-\frac{dN}{dt} = K_d \frac{(A - A_P)}{V}(N^2) \quad \text{.....(5)}$$

Integration yields

$$\frac{1}{N_t} - \frac{1}{N_0} = K_d \frac{(A - A_P)}{V} t \quad \text{.....(6)}$$

where, K_d = apparent desorption rate constant

When the values of $[1/N_t - 1/N_0]$ were plotted against $[((A - A_P)/V) \cdot t]$ values, a linear relationship was not obtained. The attempt to test for a first order reaction was also not successful, failing which the desorption rate was estimated using Eq. (7) and plotted against $(1 - \theta)$ values as shown in **Fig. 12**.

$$\text{Desorption rate} = \frac{[N_{max}] - [N_f]}{[(A - A_P)/V] \cdot t}, \quad (\%\text{-m} \cdot \text{s}^{-1}) \quad \text{.....(7)}$$

In view of the above and the increasing desorption rate (Fig. 12) with lower free sites $(1 - \theta)$ associated with high SAEs content requires explanation. It is now relevant to recall that the present experiments show heavy bubbling of the melt during plasma arc exposure.

It is generally known that in gas supersaturated melts, the gas bubbles can form. The presence of heterogeneities, such as solid particles in melt or even the solid crucible surface can act as nucleation sites for such bubble formation.

Szekely and Themelis[50] have given an approximate relationship for estimating the radius (R) of a gas bubble formed in such melts:

$$R = 2\beta\sqrt{Dt} \quad \text{.....(8)}$$

where, D = Diffusivity of nitrogen in melt

t = Time

$$\beta = \text{Growth constant} = \frac{N_s - N_e}{\rho_g} \quad \text{.....(9)}$$

where, N_s: nitrogen concentration in supersaturated melt,

N_e: equilibrium nitrogen concentration in melt,

ρ_g: gas density.

The growing gas bubble is supposed to remain attached to the nucleating surface sites till buoyancy force equals the surface tensional force. The diameter of the bubble at the time of detachment is given by Fritz formula[51]

$$d_b = 0.015\theta\left[\frac{2\sigma}{(\rho_l - \rho_g)g_c}\right]^{1/2} \quad \text{.....(10)}$$

where, θ: contact angle in degree,

σ: surface tension in between liquid and gas,

ρ_l and ρ_g: mass density of liquid and gas, respectively,

g_c: gravitational constant.

The frequency of bubble formation (f) is reciprocal of bubble growth time (t_g)

$$f = \frac{1}{t_g} = \frac{16D}{d_b^2}\frac{(N_s - N_e)^2}{\rho_g^2} \quad \text{.....(11)}$$

From the above, it is clear that the bubble diameter is directly proportional to the surface tension of the liquid which, inturn, is inversely proportional to the bubble frequency (or desorption rate). Halden and Kingery[52] have reported that SAEs lower the surface tension of liquid iron. Whalen *et al.*[53] showed that though C and Cr do not behave as SAEs but when they are present together in Fe–Cr–C alloys, they reportedly lower the surface tension of the melt due to formation of CrC complex. Unfortunately, no information is available about melt behaviour in Fe–Cr–S system. However, the present results indicate that probably the surface tension of the melt is reduced by increasing SAE in the Fe–Cr–Ni–C system. The reduced surface tension of the melt on account of higher SAE content can reduce the bubble diameter and enhance the bubble formation frequency resulting in rapid nitrogen evolution. **Figure 13** indicates increased nitrogen desorption rate with SAE in our melts and the desorption rate is also found to increase with higher sulphur and/or oxygen contents.

The melt surface tension is also affected by its temperature according to equation[11]

$$\sigma = \sigma_M[1 - \alpha(T - T_M)] \quad \text{.....(12)}$$

where, σ: surface tension at T°C,

σ_M: surface tension at melting temperature (T_M°C),

α: constant.

According to Eq. (12) the surface tension of liquid (σ) is reduced with increase in melt temperature (T°C). **Figure**

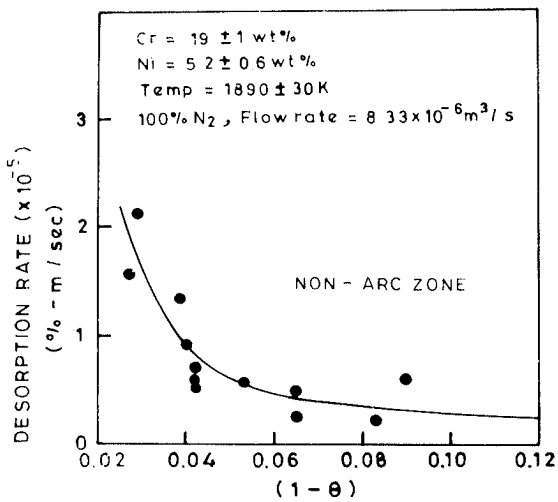

Fig. 12. Effect of free active sites on desorption rate in non-plasma arc zone.

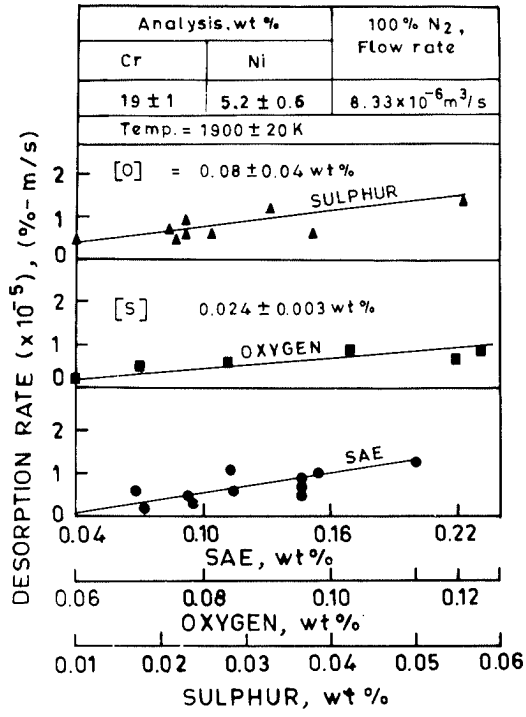

Fig. 13. Effect of SAE (sulphur and oxygen) on desorption rate of the melt.

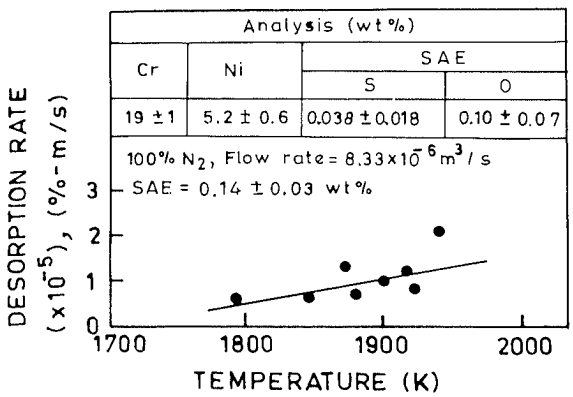

Fig. 14. Effect of melt temperature on desorption rate of the melt.

14 shows that the desorption rate increases with melt temperature (for nearly constant SAE). Thus, we conclude that low melt temperature is conducive for minimising the desorption rate in the melt.

4.4. Control of Melt Nitrogen

The process of nitrogen adsorption/desorption in melt under nitrogen plasma arc appears to be complex in view of the varied observations made by earlier researchers and in this investigation. Due to limited number of observations, it is difficult to propose any definite mechanism of gas adsorption and desorption. However, an attempt has been made to present a qualitative understanding based on the observations of this study.

The foregoing discussion on nitrogenation by plasma arc reveals that the melt nitrogen content is a balance of nitrogen adsorbed and desorbed.

Katz and King[26] and Dembovsky[38] proposed that nitrogen plasma arc contains nitrogen in atomic and ionic form, which are rapidly adsorbed by the melt surface in thermal boundary zone of the arc. This adsorbed nitrogen is then dissolved in the melt which is transported to bulk metal. The melt surface in plasma arc zone is supersaturated with nitrogen, which is the driving force for the diffusion of nitrogen to the bulk melt.

The dissolution of dissociated gas differs from that of molecular gases in one vital respect; the gas atoms are directly adsorbed and the dissociation step occurring in case of molecular gas absorption is eliminated. Thus, the process comprises four steps;

(1) Diffusion of $N_{(at)}$ in plasma arc
(2) $N_{(at)} \rightarrow N_{(ads)}$ at the thermal boundary
(3) $N_{(ads)} \rightarrow [N]$ at the metal boundary
(4) Diffusion of [N] to the metal bulk

where, $N_{(at)}$, $N_{(ads)}$, [N] are atomic, adsorbed and dissolved nitrogen.

The concentration of nitrogen in melt increases with plasma gas exposure time where temperature is also increasing. The supersaturation of melt with nitrogen leads to nucleation of nitrogen gas bubbles particularly at the lining surface (rammed in MgO). The rough MgO lining surface is believed to provide sites for gas bubble formation in the nitrogen saturated melt. The desorption through bubbles is further enhanced with increasing melt temperature.

Such bubble formation when suppressed by either application of high pressure,[23] melt stirring,[19] or using smooth crucible surface,[23,26] the desorption of nitrogen is not significant and hence, melts with high nitrogen are obtained. In cases,[19,23,26] where gas bubble formation was minimised, desorption can occur essentially by chemically controlled surface reactions inhibited by high SAE. In such studies, the presence of sulphur, though beneficial in getting higher nitrogen content, cannot be used in practice due to its deleterious effects[45] on metal quality.

The present experimental method offers an advantageous condition whereby the low SAE level in the melt renders higher absorption rate* (**Fig. 15**) and low desorption rate (Fig. 13) which is ideal to produce melt with high nitrogen and low SAE required in practice.

5. Conclusions

In light of this work, some guidelines can be suggested to prepare Fe–Cr alloys containing nitrogen.

(1) Since nitrogen level in the products has been found to increase with Cr and Mn contents and decreases with increased Ni, it is recommended that steels with higher levels of the former with minimal amount of the latter be produced using the plasma arc nitrogenation technique.

(2) The melt nitrogen is a balance of nitrogen absorbed and desorbed in a given time. Hence conditions

* Absorption rate $= \dfrac{[N_{max}]-[Ni]}{(A_p/V)t}$ (%-m·s^{-1}) ..... (13)

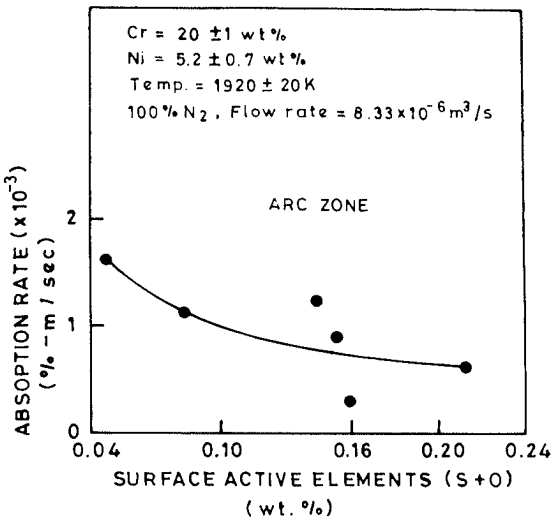

Fig. 15. Effect of SAE on absorption rate in plasma arc zone.

which promote absorption and retard desorption have to be used.

The nitrogen absorption occurring in plasma arc zone appears to be controlled by 1st order chemical reaction rate. Whereas, nitrogen desorption appears to occur *via* bubble formation, the frequency of which appears to depend on SAE.

Therefore, lower SAE in the melt [enabling higher absorption (or adsorption) rate – Fig. 15 and slower desorption rate – Fig. 13] can yield higher melt nitrogen content (Fig. 7).

(3) In order to aim at definite nitrogen content in the melt, it is essential to estimate the correct plasma gas exposure time. With the present experimental set up, it was necessary to stop the plasma gas exposure before the rate of desorption exceeds the rate of absorption (or adsorption) as noticed in Fig. 2. If this desorption is being controlled by bubble formation then it is necessary to study the bubble formation frequency as affected by process parameters. In all the melts of this work, it was noted that desorption process dominantes only after 120–180 s exposure time.

Acknowledgements

The authors wish to thank Prof. P. M. Prasad, Department of Metallurgical Engineering, Institute of Technology, Banaras Hindu University for discussion and suggestions. Thanks are also due to Prof. K. M. Pai, Indian Institute of Technology, Bombay for his help in chemical analysis.

REFERENCES

1) W. B. Morrison: *Ironmaking Steelmaking*, **16** (1989), No. 2, 123.
2) T. P. Battle and R. D. Pehlke: *Ironmaking Steelmaking*, **13** (1986), No. 4, 176.
3) W. D. Cho and Y. K. Rao: *Ironmaking Steelmaking*, **17** (1990), No. 4, 261.
4) M. Sano, K. Kadoguchi and K. Mori: *Trans. Iron Steel Inst. Jpn.*, **24** (1984), No. 10, 825.
5) M. Takahashi, H. Matsuda, M. Sano and K. Mori: *Trans. Iron Steel Inst. Jpn.*, **27** (1987), No. 8, 626.
6) M. Takahashi, M. Sano, K. Mori and M. Hirasawa: *Trans. Iron Steel Inst. Jpn.*, **27** (1987), No. 8, 633.
7) S. V. Gallardo, D. N. Hawkins and J. Beech: Dept. Metall., Sheffield University, UK, personal communication, (1988).
8) H. G. Lee and Y. K. Rao: *Ironmaking Steelmaking*, **12** (1985), No. 5, 221.
9) Y. K. Rao and H. G. Lee: *Ironmaking Steelmaking*, **12** (1985), No. 5, 209.
10) R. D. Pehlke and J. F. Elliott: *Trans. AIME*, **227** (1963), 844.
11) M. Inouye and T. Choh: *Trans. Iron Steel Inst. Jpn.*, **8** (1968), No. 3, 134.
12) R. J. Fruehan and L. J. Martonik: *Metall. Trans. B*, **11B** (1980), No. 4, 615.
13) M. Inouye and T. Choh: *Trans. Iron Steel Inst. Jpn.*, **12** (1972), No. 3, 189.
14) R. J. Fruehan and L. J. Martonik: *Metall. Trans. B*, **12B** (1981), 379.
15) J. H. Swisher and E. T. Turkdogan: *Trans. AIME*, **239** (1967), No. 5, 602.
16) C. H. Hua and N. A. D. Parlee: *Metall. Trans. B*, **13B** (1982), 357.
17) L. A. Greenberg and A. McLean: *Ironmaking Steelmaking*, **9** (1982), No. 2, 58.
18) K. Shimmyo and T. Takami: Proc. Int. Conf. Science and Technology of Iron and Steel, ISIJ, Tokyo, (1971), 543.
19) F. L. Kemeny, A. McLean and I. D. Sommerville: Electric Furnace Conference Proc., Vol. 45, ISS-AIME, Chicago, USA, (1987), 285.
20) Y. K. Rao and H. G. Lee: *Ironmaking Steelmaking*, **15** (1988), No. 5, 228.
21) K. Ito, K. Amano and H. Sakao: *Trans. Iron Steel Inst. Jpn.*, **28** (1988), No. 1, 41.
22) Y. K. Rao and W. D. Cho: *Ironmaking Steelmaking*, **17** (1990), No. 4, 273.
23) K. Takeda and Y. Nakamura: *Trans. Iron Steel Inst. Jpn.*, **18** (1978), No. 10, 641.
24) T. E. Gammel, G. Hinds and I. Mokrov: Proc. of 6th Vacuum Metallurgy Conference on Special Melting; Sandiego, California, (1979), 1.
25) J. D. Katz and Late T. B. King: *Trans. Iron Steel Inst. Jpn.*, **28** (1988), No. 5, 360.
26) J. D. Katz and T. B. King: *Metall. Trans. B.*, **20B** (1989), No. 2, 175.
27) T. Knopper: *Iron Steel Eng.*, **62** (1985), No. 5, 23.
28) D. Neuschutz, H. O. Rossner, H. J. Bebber and J. Hartwig: *Iron Steel Eng.*, **62** (1985), No. 5, 27.
29) I. D. Sommerville, A. McLean, C. B. Alcock and C. A. Pickles: Plasma Technology in Metallurgical Processing, ed. by Jorme Feinman, Iron and Steel Society, Warrendale, USA, (1987), 89.
30) R.C. Eschenback, N. A. Barcza and K. J. Reid: Plasma Technology in Metallurgical Processing, ed. by Jorme Feinman, Iron and Steel Society, Warrendale, USA, (1987), 77.
31) O. P. Sinha and R. C. Gupta: *Tool Alloy Steels*, **14** (1990), No. 12, 463.
32) G. F. Torkhov, Yu. V. Latash, R. R. Fessler, A. H. Claver, E. E. Fletcher and A. L. Hoffmanner: *J. Met.*, **30** (1978), No. 12, 20.
33) P. Rama Rao and V. V. Kutumbarao: *Int. Mater. Rev.*, **34** (1989), No. 2, 69.
34) R. P. Reed: *J. Met.*, **41** (1989), No. 3, 16.
35) R. C. Gupta and O. P. Sinha: *Tool Alloy Steels*, **23** (1989), No. 9, 333.
36) B. R. Nijhawan, P. K. Gupta, S. S. Bhatnagar, B. K. Guha and S. S. Dhanjal: *J. Iron Steel Inst.*, **204** (1967), No. 3, 292.
37) O. P. Sinha and R. C. Gupta: Conference on High Temperature Materials Properties, France, June 17–20, (1991).
38) Vladimir Dembovsky: Plasma Metallurgy—The Principles, Elsevier, Amsterdam, (1985), 321.
39) P. D. Blake and M. F. Jordan: *J. Iron Steel Inst.*, **209** (1971), No. 3, 197.
40) F. S. Death and D. A. Haid: V.S. Patent 3.257.197 (1966).
41) G. K. Bhatt: Plasma Technology in Metallurgical Processing, ed. by Jorme Feinman, Iron and Steel Society, Warrendale, USA, (1987), 163.
42) R. G. Ward: An Introduction to the Physical Chemistry of Iron

and Steelmaking, Edward Arnold Publisher Ltd., London, (1962), 175.
43) R. D. Pehlke and J. F. Elliott: *Trans. AIME*, **218** (1960), No. 2, 1088.
44) A. R. Perrin, M. Wolosiuk and A. McLean: *Trans. ISS*, **14** (1987), No. 6, 45.
45) O. P. Sinha, A. K. Singh, C. Ramchandra and R. C. Gupta: *Metall. Trans. A*, **23A** (1992), No. 12, 3317.
46) M. B. Donald and H. Singer: *Trans. Inst. Chem. Eng.*, **37** (1959), 255.
47) S. Corrsin and M. S. Uberoi: NACA TN 1865, US Government, Printing Office, Washington, DC, (1953).
48) J. Szekely and N. J. Themelis: Rate Phenomena in Process Metallurgy, Wiley-Inter Science, New York, London, (1971), 720.
49) M. Byrne and G. R. Belton: *Metall. Trans. B.*, **14B** (1983), No. 3, 441.
50) J. Szekely and N. J. Themelis: Rate Phenomena in Process Metallurgy, Wiley-Interscience, New York, London, (1971), 684.
51) W. Fritz: *Physik*, **36** (1965), 379; Rate Phenomena in Process Metallurgy, Wiley-Interscience, New York, London, (1971), 452.
52) F. A. Halden and W. D. Kingery: *J. Phys. Chem.*, **59** (1955), 557.
53) T. J. Whalen, S. M. Kanfman and M. Humenik: *Trans. ASM*, **55** (1962), 778.